Applied Clay Science 151 (2018) 102–108

Contents lists available at ScienceDirect

Applied Clay Science

journal homepage: www.elsevier.com/locate/clay

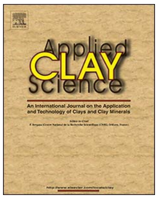

Research paper

Study on non-darcian flow sand-clay mixtures

Shengwei Wang[a,*], Wei Zhu[b,c,d], Kang Fei[a], Chaoyang Xu[a], Nan Zhang[e]

[a] *Institute of Geotechnical Engineering, Yangzhou University, Yangzhou 225127, China*
[b] *Key laboratory of Ministry of Education for Geomechanics and Embankment Engineering, Hohai University, Nanjing 210098, China*
[c] *Jiangsu Research Center for Geotechnical Engineering Technology, Hohai University, Nanjing 210098, China*
[d] *College of Environment, Hohai University, Nanjing, China*
[e] *Department of civil engineering, University of Texas at Arlington, TX, USA*

ARTICLE INFO

Keywords:
Sand-clay
Hydraulic conductivity
Intrinsic permeability
Threshold gradient
Modified effective aperture

ABSTRACT

Compacted clay liners in landfills can easily develop fissures in a dry environment. To overcome this, sand is added to the clay. In this study, various mixes of sand-clay soils were tested for their hydraulic conductivity, threshold gradient, as well as bound forms of pore water. The water flow behavior in the sand-clay samples varied according to the sand content. When the sand content was no $<$ 50%, the compacted sand-clay permeability conformed to Darcy's law. When the sand content was $>$ 50%, the permeability deviated from Darcy's law and a threshold gradient became apparent. The lowest hydraulic conductivity was measured in the sand-clay sample with 30% sand content. Based on the seepage theory, the relation between the sand content and the soil's intrinsic permeability was obtained and a model representing the relation between the sand content and hydraulic conductivity was established. Based on analysis of the water morphology between the soil particles, the Hange-Poiseuille law was modified, showing that changing the sand content of the sand-clay can modify the effective apertures of the soil. When the sand content was 30%, the modified effective aperture was the smallest, which explains why the hydraulic conductivity was smallest and the threshold gradient was largest. Considering the empirical relationship between the modified effective aperture and threshold gradient derived in previous studies, this paper furthers our understanding of the development of the threshold gradient in sand-clay soils.

1. Introduction

Water plays an important role in the penetration process of substances through low-permeability materials. For instance, because of its low permeability, geo-engineers use clay as a barrier to confine high-level radioactive waste (Tsang et al., 2012). Compacted clay is also important as a liner in landfills (Koutsopoulou et al., 2010; Xue et al., 2013; Wang et al., 2017). When constructing liners for landfills in arid areas, fissures may form in compacted clays because of the dry conditions. A fissure network can develop rapidly, leading to more loss of water and deeper fissures (Hewitt and Philip, 1999). Fissures will worsen the liner's anti-permeability. The preferential pathway created by the fissures will speed the leachate leakage, polluting the groundwater and the surrounding environment.

Clay often has high shrinkage, which promotes the formation of dry fissures. To reduce shrinkage, sand is added to the clay (Wanrong and Guo, 2000). To improve sand-clay liners, studies were conducted on the influence of sand on the workability (Danbing et al., 2016), liquid limit (Park and Nong, 2014; Cabalar and Mustafa, 2015) and hydraulic conductivity (Sivapullaiah et al., 2000; Yeo et al., 2005; Zhang et al., 2016) of clay-sand soils. Xu et al. (2016) mixed sand and clay in different proportions and investigated the permeability of the various samples. The hydraulic conductivity of sand-clay mixtures decreased as the clay content increased up to a certain point, and then the conductivity gradually decreased.

The leachate head in some Chinese landfills can be very high, over 10 m in some cases (Chen and Zhan, 2007); therefore, Wang et al. (2016) suggested including a threshold gradient for compacted clay liners to prevent high leachate leakage. To ensure that sand-clay barriers act as anti-pollution barriers, it is important to evaluate their threshold gradient. However, research related to this subject is scarce. Many studies that examined the threshold gradient generated by sand-clay soils found that it was related to the water morphology between the soil particles. Florin (1951) noted that the bound water retained by the surface force of the soil particles did not flow in narrow and long pores. This effect could block the flow of free water. Only when the driving gradient was large enough to destroy the bound water, could water flow occur. Miller and Low (1963) found a “quasicrystal” structure in the interface of the clay and water and proposed that seepage is caused by a shear stress that deforms the water membrane structure.

---

[*] Corresponding author at: No.196, Huayang West Road, Hanjiang District, Yangzhou 225127, China.
E-mail address: dvlove2007@126.com (S. Wang).

http://dx.doi.org/10.1016/j.clay.2017.10.028
Received 17 April 2017; Received in revised form 18 October 2017; Accepted 21 October 2017

Liu and Birkholzer (2012) summarized previous research results of both fully and partially saturated clays and established a relationship between permeability and the threshold gradient. They found that the threshold gradient increased with decreased permeability. Singh and Wallender (2008) adopted the modified Kozeny–Carman equation to predict hydraulic conductivity. It is known that water films on the surface of clay particles cannot flow under a hydraulic gradient. When this part of the pore water was removed and the remaining was used as effective pores to modify the Kozeny–Carman equation, reliable estimates of hydraulic conductivity were obtained. Wei et al. (2009) performed mercury injection experiments and permeability tests at the Daqing Oil Field. The authors first obtained the aperture distribution curve by using the mercury injection experiment and then defined the value of 95% at the curve as the mainstream throat radius. Many scholars used nanotubes to simulate the clay pores, and applied molecular dynamics to study the flow process in the nanotubes. They showed that the flow in macropores was quite different from that in micropores, and the water density near the particle surface was greater than that of free water (Chen et al., 2008; Farrow et al., 2011).

Compacted clay can easily produce fissures in a dry environment during landfill construction, which forms preferential seepage pathways. To overcome this problem, sand is added to the clay to produce an effective anti-pollution barrier. Because of high leachate water levels, it is important to confirm whether a sand-clay anti-pollution barrier can produce a threshold gradient, and determine the sand content needed to provide the maximum gradient level. In the work described in this paper, water flow in soils with different sand-clay proportions is examined and the effect of the sand content on the hydraulic conductivity and threshold gradient are discussed. The water morphology between the soil particles is also analyzed and the formation of the threshold gradient in sand-clay mixtures is discussed.

2. Materials and methods

2.1. Materials

Since soil formations vary greatly depending on site conditions, Chinese Fujian standard sand (Sand-F) was used to simulate the sandy soil layer at the site. The basic physical properties of Sand-F are listed in Table 1.

The clay produced in Jiangning District of Nanjing, China (called as Clay-J). X-ray diffraction analysis of Clay-J was conducted by a Rigaku D/max-rC rotating anode X-ray powder diffractometer. Air-dried powdered samples (particle size < 75 μm) of Clay-J was used. The X-ray source was a Cu anode operating at 40 kV and 100 mA using Cu Kα radiation (λ = 1.5406 Å). The run speed was 3°/min. Data were collected between 5° and 40° in 2θ increments (Mitchell and Soga, 2005). The mineralogical analysis of the X-ray diffraction pattern of Clay-J was conducted by comparing with the X-ray powder diffraction standard files (Joint Committee for Powder Diffraction Standards, 1995). The mineralogical characterizations by X-ray diffraction of Clay-J is shown in Fig. 1.

Based on the X-ray diffraction analysis, the main clay minerals were identified as illite (basal order reflections = 10.18 Å, 4.99 Å, 3.67 Å, 2.56 Å); montmorillonite (basal order reflections = 14.52 Å, 4.48 Å, 3.50 Å); quartz (basal order reflections = 4.26 Å, 3.35 Å, 2.46 Å, 2.28 Å); and anorthite (basal order reflections = 4.03 Å, 3.77 Å, 3.20 Å, 2.93 Å). The liquid limit (LL), plastic limit (PL) and specific gravity (G_s) were measured according to the GB/T 50123–1999 method (China, 1999). From the relationship established between the soil water content and the cone penetration depth, the water content corresponding to a depth of 17 mm is the liquid limit, and that corresponding to a depth of 10 mm is the plastic limit. The zeta potential of the Clay-J dispersion system containing 0.5% solids in distilled water was determined by micro electrophoresis using a Malvern Zetasizer Nano zeta potential analyzer. The particle size distribution curves for the Clay-J and Sand-F samples are shown in Fig. 2. The particle-size distribution of Clay-J was measured by using a laser particle-size analyzer Mastersizer 2000. According to the Unified Soil Classification System (ASTM, 2011), Sand-F is poorly graded sand (SP) and Clay-J is clay (CL) with low plasticity. The cation exchange capacities (CEC) of the materials were determined using the JC/T593–1995 method (State Construction Materials Industry Administration, 2004). The interchangeable Calcium and Magnesium were measured by the ammonium acetate exchange-EDTA complexometric titration method. The interchangeable Potassium and Sodium was tested by the ammonium acetate exchange-flame photometry rule. The index properties were presented in Table 2. Ordinary deionized water was used in the tests.

Table 1
Physical properties of Fujian standard sand.

G_s	C_u	ρ_{dmax} (g/cm^3)	ρ_{dmin} (g/cm^3)	e_{max}	e_{min}
2.64	5.99	1.74	1.43	0.85	0.52

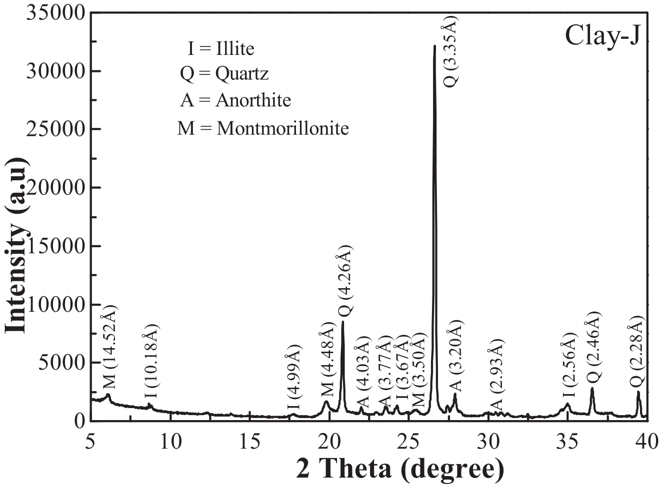

Fig. 1. X-ray diffraction patterns for Clay-J.

2.2. Sample preparation

The two types of soil were air-dried; the clay was crushed and sieved using 1-mm sieves. The clay and sand were mixed and deionized water was added and the mixture was stirred thoroughly. The Clay-J content

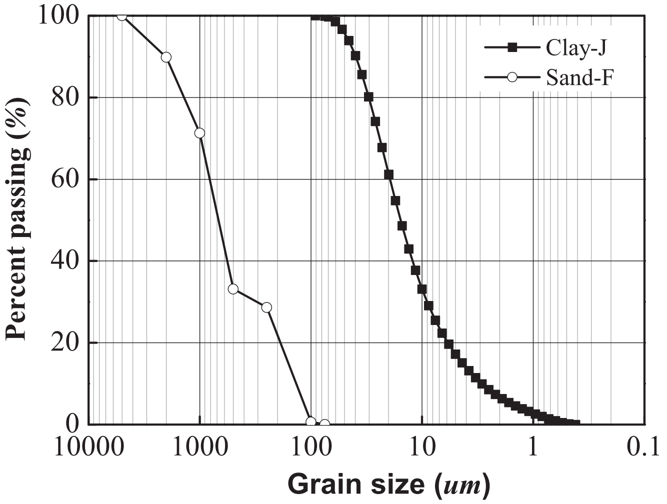

Fig. 2. Grain size distribution curves.